NeuroImage 129 (2016) 439–449

Contents lists available at ScienceDirect

NeuroImage

journal homepage: www.elsevier.com/locate/ynimg

Full Length Article

Underlying sources of cognitive-anatomical variation in multi-modal neuroimaging and cognitive testing

P.D. Watson [a,*], E.J. Paul [a], G.E. Cooke [a], N. Ward [a], J.M. Monti [a], K.M. Horecka [a,h], C.M. Allen [a], C.H. Hillman [a,b], N.J. Cohen [a,c], A.F. Kramer [a,c], A.K. Barbey [a,c,d,e,f,g,h,*]

[a] Beckman Institute for Advanced Science and Technology, University of Illinois at Urbana–Champaign, Urbana, IL, USA
[b] Department of Kinesiology and Community Health, University of Illinois at Urbana–Champaign, Urbana, IL, USA
[c] Department of Psychology, University of Illinois at Urbana–Champaign, Champaign, IL, USA
[d] Decision Neuroscience Laboratory, University of Illinois at Urbana–Champaign, Champaign, IL, USA
[e] Department of Bioengineering, University of Illinois at Urbana–Champaign, Urbana, IL, USA
[f] Department of Internal Medicine, University of Illinois at Urbana–Champaign, Champaign, IL, USA
[g] Department of Speech and Hearing Science, University of Illinois at Urbana–Champaign, Champaign, IL, USA
[h] Neuroscience Program, University of Illinois at Urbana–Champaign, Champaign, IL, USA

ARTICLE INFO

Article history:
Received 17 August 2015
Accepted 11 January 2016
Available online 22 January 2016

ABSTRACT

Healthy adults have robust individual differences in neuroanatomy and cognitive ability not captured by demographics or gross morphology (Luders, Narr, Thompson, & Toga, 2009). We used a hierarchical independent component analysis (hICA) to create novel characterizations of individual differences in our participants (N = 190). These components fused data across multiple cognitive tests and neuroanatomical variables. The first level contained four independent, underlying sources of phenotypic variance that predominately modeled broad relationships within types of data (e.g., "white matter," or "subcortical gray matter"), but were not reflective of traditional individual difference measures such as sex, age, or intracranial volume. After accounting for the novel individual difference measures, a second level analysis identified two underlying sources of phenotypic variation. One of these made strong, joint contributions to both the anatomical structures associated with the core fronto-parietal "rich club" network (van den Heuvel & Sporns, 2011), and to cognitive factors. These findings suggest that a hierarchical, data-driven approach is able to identify underlying sources of individual difference that contribute to cognitive-anatomical variation in healthy young adults.

Published by Elsevier Inc.

Introduction

Every brain is unique. These differences in brain structure and physiology contribute to the stunning diversity of human thought and identity. Magnetic resonance imaging (MRI) scanning and post-processing techniques provide a new window on individual differences, characterizing volume, cortical thickness, and white-matter integrity. Further, these techniques categorize the massively multivariate raw MRI images into a set of robust and meaningful summary variables tied to brain health or function rather than performance on a specific task.

Extensive literature focuses on the complex network of interactions between sex, age, cognitive factors, brain size and shape, gray matter, education, fitness, and a host of other variables (Gray et al., 2003; Rypma and Prabhakaran, 2009; Goh et al., 2011). One way to approach this complex series of interactions is as a source separation problem: the many manifest variables are a phenotype produced by mixing of smaller number of underlying sources of variation. Identifying the underlying sources could help discover and differentiate anatomical brain phenotypes. Building a model of these sources would allow us to better control for individual variation and to identify how brain measures cluster at multiple levels of specificity.

However, finding joint contributions to anatomical and cognitive variables in MRI image sets has been challenging, especially in healthy young adults (Haier et al., 2004; Luders et al., 2009; McDaniel, 2005; Wickett et al., 2000). Such relationships are often limited to broad morphological effects such as a correlation between brain size and fluid intelligence (gf; McDaniel, 2005), or are characterized more in special populations with greater individual brain variation such as in older adults (Goh et al., 2011).

Yet lesion studies robustly link cognitive factors to anatomy (Allen et al., 2006; Barbey et al., 2012; Barbey et al., 2014), as do functional and resting state imaging (Buckner et al., 2008; Von den Heuvel and Sporns, 2011; Wang et al., 2013). Specific anatomical hypotheses

* Corresponding authors at: Decision Neuroscience Laboratory, Beckman Institute for Advanced Science and Technology, University of Illinois at Urbana-Champaign 405 North Mathews Avenue Urbana, IL 61801, USA.
E-mail addresses: pwatson1@illinois.edu (P.D. Watson), barbey@illinois.edu (A.K. Barbey).
URL: http://DecisionNeuroscienceLab.org/ (P.D. Watson).

http://dx.doi.org/10.1016/j.neuroimage.2016.01.023
1053-8119/Published by Elsevier Inc.

developed from such data, the parieto-frontal integration theory (PFIT), maps high-level cognitive factors such as fluid intelligence to a network of superior parietal and frontal regions that integrate multiple sources of information in service of a goal (Jung and Haier, 2007). A parallel framework maps these functions to a highly functionally interconnected "rich club" of fronto-parietal regions (Van den Heuvel and Sporns, 2011). Why aren't these sources readily apparent as variation in individual anatomical data?

There are converging reasons that joint sources of cognitive and anatomical variation could be difficult to identify. Anatomical scans lack the robust time-series data of functional scans, and thus cognitive-anatomical relationships require larger sample sizes to assess effects. Additionally, the hypothesized fluid intelligence network is distributed across multiple anatomical regions and tissue types (e.g., gray vs. white matter) best assessed by different imaging methods (e.g., T1 weighted scans v. diffusion tensor imaging). Thus, the common variation associated with these functional networks is likely distributed throughout multiple regions and imaging modalities and might not pass statistical thresholds in any single region, let alone across all regions of the entire network. Finally, there might be different relationships between anatomy and cognitive factors at different levels of analysis: with strong, low-level sources of anatomical variability obscuring more subtle signals tying cognitive functions to anatomical networks.

In the current paper, we employ a hierarchical independent component analysis (hICA) to fuse 124 measures of phenotypic variance across cognitive, neuroanatomical, and demographic values assessed in 190 healthy adults. Similar approaches have been used before to fuse functional data (Groves et al., 2011; Laird et al., 2011; Smith et al., 2009; Sui et al., 2011, 2012). We compare variation across four types of MRI-assessed individual difference measures (cortical and subcortical volumes, cortical thickness, white-matter integrity), and a battery of demographic, fitness, and cognitive measures. This first-level ICA serves to identify sources of phenotypic variation that make joint contributions to multiple cognitive factors and multiple regions and types of brain anatomy. We then regress these first-level components from our data and perform ICA on the residual correlations in our data, to produce second-level components that describe additional sources of cognitive-anatomical variation, but were not well captured in the first-level analysis.

By examining the anatomical maps of these independent sources of variation, and exploring their relationships with specific cognitive factors, we hope to better characterize underlying sources of variation that jointly contribute to anatomical and cognitive variations across multiple levels. As a test-case, we also examine how these high-level factors relate to PFIT "rich club" network hypothesized to be related to general intelligence including higher cognitive functions such as fluid intelligence (Colom et al., 2009; Jung and Haier, 2007).

Methods

Sample

Participants were recruited from East-Central Illinois for the INSIGHT ("An integrative system for enhancing fluid intelligence through human cognitive activity, fitness, brain stimulation, and nutritional intervention") study. All participants received a battery of 12 cognitive tests and a fitness assessment. Half of these individuals received an additional battery of anatomical and functional MRI scans. Excluding individuals with incomplete data, our total sample is 518 individuals (239 females, mean age: 24.3 years) with cognitive and fitness assessments, of whom 190 had complete imaging data (i.e., we excluded any individual missing any of the measures assessed by our analysis). The independent component analyses presented here include only this imaging sub-set of the total sample.

To confirm that this sample was representative of the larger dataset from which the factor scores were computed we performed a one-way ANOVA (imaging group v. full sample) and found no significant between-group differences on age, sex, education or any of the four cognitive factors (d.f. = 2515, all F values between 0 and 2.1, all $p > .12$).

Demographics

The 190 participants consisted of 85 females, and 105 males. The age range in our sample was 18–44 years, with a median of 22 years, and a mean of 24.3 years. The mean educational level of the participants was "some college" (i.e., median score 3, mean score 3.6) as reported on a scale from 1 to 5, where 1 denoted "less than a high school diploma", 2 denoted "high school diploma or equivalent", 3 denoted "some college", 4 denoted "college degree", and 5 denoted "post-graduate education." (See Table 1)

Aerobic fitness assessment

Cardiovascular fitness has previously been shown to have important contributions to neural health and cognitive function (Kramer et al., 2001, 2005). Maximal oxygen consumption (VO_{2max}) was measured using a computerized indirect calorimetry system (ParvoMedics True Max 2400) and a modified Balke protocol (American College of Sports Medicine. ACSM's Guidelines for Exercise Testing and Prescription, 2014) with averages for oxygen uptake (VO_2) and respiratory exchange ratio (RER) assessed every 20 s. Participants ran on a motor-driven treadmill at a constant speed, with 2.0% increases in grade every 2 min until volitional exhaustion. The raw value was adjusted for body size, age, and gender to produce a VO_{2max} percentile score.

Cognitive tests and factor scores

Participants received a battery of 12, standardized cognitive tests designed to estimate underlying latent variables corresponding to cognitive constructs (see Table 2). The four latent variables of interest were fluid intelligence (gf), working memory (wm), executive function (ef), and episodic memory (em).

Procedures for these tests are described in detail in the associated citations. Brief descriptions are as follows: The BOMAT is an untimed, thirty-item matrix-reasoning test. Number series involves generating the next element in a string of numbers related by a common function. In letter sets, participants pick which of five sets of four letters differs from the others. Reading, rotation, and symmetry span are all complex span tasks, involving holding items in working memory while processing intervening distractors. The target items are words, arrows of different lengths and angles, and the locations of elements in a grid. Garavan involves keeping track of multiple internal counts, and measures errors in counts and the cost of switching between them. Keep track involves viewing an array of categories, and then identifying and remembering words belonging to those categories. Stroop involves identifying the color a word is printed in while inhibiting reading of the word. All three episodic memory tasks involve timed study of a list of words, pictures, or paired associates (respectively), and are scored by the number of items a participant can produce immediately after study.

Using a structural equation modeling approach (Kane et al., 2004), across the larger sample of 518 participants, we extracted estimates of the four cognitive construct latent variables (i.e., gf, wm, ef, em).

Table 1
Demographics.

	Imaging sample (N = 190)	Full sample (N = 518)
% Female	45%	50%
Mean age (std)	24.3 (6.6)	24.3 (6.0)
Mean education (std)	3.5 (0.9)	3.5 (0.8)

Table 2
Cognitive tests.

Latent variable	Test name	Measure	Detailed description
Fluid intelligence (gf)	BOMAT matrix reasoning	Correct trials	Bocumer Matrizentest: BOMAT-advanced-short Version (2009)
	Number series	Correct trials	Bernreuter and Goodman (1941)
	Letter sets	Correct trials	Ekstrom et al. (1976)
Working memory (wm)	Reading span	Total span	Engle et al. (1999a)
	Rotation span	Total span	Shah and Miyake (1996)
	Symmetry span	Total span	Unsworth et al. (2009)
Executive function (ef)	Garavan	Total errors	Garavan (1998)
	Keep track	Words recalled	Yntema (1963)
	Stroop	Stroop effect	Stroop (1935)
Episodic memory (em)	Immediate free recall words	Words recalled	Engle et al. (1999b)
	Immediate free recall pictures	Pictures recalled	Unsworth et al. (2009)
	Immediate free recall paired associates	Pairs recalled	Uttl et al. (2002)

Because Garavan and Stroop produce error scores, while all others are measures of accuracy, we inverted these two values (i.e., multiplied by −1) in order to ensure all cognitive variables had the same sign.

Structural MRI protocol

High resolution T1-weighted brain images were acquired using a 3D MPRAGE (Magnetization Prepared Rapid Gradient Echo Imaging) protocol with 192 contiguous axial slices, collected in ascending fashion parallel to the anterior and posterior commissures, echo time (TE) = 2.32 ms, repetition time (TR) = 1900 ms, field of view (FOV) = 230 mm, acquisition matrix 256 mm × 256 mm, slice thickness = 0.90 mm, and flip angle = 9°. All images were collected on a Siemens Magnetom Trio 3T whole-body MRI scanner.

Automated volumetrics, cortical thickness estimates, and white-matter tractography

Automated brain tissue segmentation and reconstruction of the T1-weighted structural MRI images were performed using the standard recon-all processing pipeline in FreeSurfer, version 5.2.0 (Released May 2013; http://surfer-nmr.mgh.harvard.edu/). This produced estimates of 1) cortical thickness, 2) cortical volumes, 3) sub-cortical volumes, 4) ventricles, and 5) corpus callosum (Dale et al., 1999; Desikan et al., 2006; Fischl and Dale, 2000; Fischl et al., 2002, 2004a, 2004b). Segmentations and tractography were manually checked for errors. Estimates in the left and right hemispheres were summed to produce bilateral estimates, and all values were converted to z-scores to control for differences in scale. A complete list of estimated structures appears in Table 3. FreeSurfer produced automated segmentation closely approximate hand tracing (Morey et al., 2009), but like all segmentation procedures may introduce systematic bias.

The diffusion tensor imaging fractional anisotropy (FA) data was analyzed using tract-based spatial statistics in FSL (Smith, 2002; Smith et al., 2004, 2006). This pipeline involves fitting a tensor model to the raw diffusion data using fMRIDB's diffusion toolbox, and non-brain tissues were removed using FSL's brain extraction tool. All subjects' FA data were then aligned into a common space using the nonlinear registration tool FNIRT (Andersson et al., 2007; Rueckert et al., 1999). Next, the mean FA image was created and thinned to create a mean FA skeleton that represents the centers of all tracts common to the group. Each subject's aligned FA data was then projected onto this skeleton to create an estimate of the subject-level value associated with each tract.

Radial diffusivity (RD) values were also obtained from this analysis. Due to the physical relationship between RD and FA values, tract-wise measures of RD and FA are all strongly negatively correlated (R values between −.44 and −.9, all $p < .001$ after Bonferroni correction). Principle component analysis (PCA) of these FA and RD values produced a single factor which accounted for 64% of the variance of the full sample, upon which all 22 FA and RD values loaded with factor scores between .55 and .95. This suggests that RD carries similar information to FA and we did not include it in the main analysis presented here, however, we did include these RD values in our follow-up validation analysis.

Grand table of multi-modal demographic, cognitive, and imaging variables

All variables measured with the above methods appear in Table 3 in the order they appear in Fig. 1.

In our follow-up analysis we also included radial diffusivity (RD) values for each of the white matter tracts reported above.

Global correlations and independent component analysis

Global correlations were computed among all variables and plotted using MATLAB (MATLAB and Statistics Toolbox Release, 2014a). First level independent components were computed using the Fast-ICA algorithm (Hyvärinen, 1999), with the number of components determined by scree plot inspection of the whitened correlation matrix (Costello and Osborne, 1994). Standardized residuals with respect to the IC factor loadings (i.e., the E matrix) were obtained by computing a general linear model (GLM) with all of the variables in Table 3 as dependent variables, and the four IC factor scores as independent variables (i.e., computing residuals across all of our measures with respect to model including only the four independent components). This GLM was computed in SPSS (IBM Corp. Released, 2013). The second-level ICA was performed on these residuals in the same fashion as the first-level. In both cases we used cross-validation in ICA extraction (Westad and Kermit, 2003). This uses a Monte-Carlo procedure that extracts IC multiple times, and checks correlation between IC components to ensure that the factors were robust to the initial conditions of the ICA algorithm.

We additionally validate these ICs by performing a follow-up analysis using a slightly different variable set (excluding the demographic variables, including the radial diffusivity variables). We report the relationship between the IC values extracted in this analysis and the IC values extracted in the main analysis.

IC projections onto brain maps

After obtaining first- and second-level ICs of brain variation in our sample, we selected a representative participant's brain segmentation, and for each region, applied the loading estimated by the IC to the voxels that fell within that segment, and then transformed the brain back into MNI space (Mazziotta et al., 1995). We overlaid these values on the MNI CSF template with a threshold corresponding to an IC score with an absolute value of 1.0 or greater. Values above this threshold correspond to variables that contribute more to the variability of the IC than to the variability of the original data set, (i.e., these are variables that inform the IC), while variables below this threshold are less informative to this IC than they are to the dataset as a whole. All four cognitive factors were plotted using the IC color map (including those

Table 3
Grand table of measured variables.

Data categories	Specific measures
Demographics & cardiovascular fitness	Age
	Years of education
	Sex
	VO_{2max} percentile
Cognition	Fluid intelligence (gf)
	Working memory (wm)
	Executive function (ef)
	Episodic memory (em)
	BOMAT (correct trials)
	Number series (correct trials)
	Letter sets (correct trials)
	Reading span
	Rotation span
	Symmetry span
	Garavan (inverse total errors)
	Keep track words recalled
	Stroop (inverse cost)
	Immediate free recall words
	Immediate free recall pictures
	Immediate free recall paired associates
Cortical thicknesses	Superior parietal
	Postcentral
	Precuneus
	Lateral occipital
	Mean cortical thickness
	Superior temporal
	Inferior parietal
	Paracentral
	Precentral
	Middle temporal
	Banks of superior temporal sulcus
	Insula
	Superior frontal
	Supramarginal
	Transverse temporal
	Rostral middle frontal
	Caudal middle frontal
	Pars triangularis
	Pars opercularis
	Lateral orbitofrontal
	Pars orbitalis
	Frontal pole
	Posterior cingulate
	Inferior temporal
	Cuneus
	Peri calcarine
	Rostral anterior cingulate
	Medial orbitofrontal
	Caudal anterior cingulate
	Isthmus cingulate
	Fusiform
	Temporal pole
	Lingual
	Entorhinal
	Parahippocampal
Cortical volumes	Middle temporal
	Inferior parietal
	Inferior temporal
	Rostral anterior cingulate
	Posterior cingulate
	Rostral middle frontal
	Superior frontal
	Precentral
	Supra marginal
	Lateral orbitofrontal
	Fusiform
	Precuneus
	Insula
	Medial orbitofrontal
	Postcentral
	Superior temporal
	Caudal middle frontal
	Paracentral
	Superior parietal
	Isthmus cingulate
	Lateral occipital
	Transverse temporal
	Pars orbitalis
	Pars opercularis
	Caudal anterior cingulate
	Pars triangularis
	Entorhinal
	Temporal pole
	Parahippocampal
	Frontal pole
	Peri calcarine
	Cuneus
	Lingual
Sub-cortical volumes	Total brain volume
	Total intracranial volume
	Hippocampus
	Ventral diencephalon
	Cerebellum cortex
	Cerebellum white matter
	Thalamus
	Brain stem
	Amygdala
	Putamen
	Accumbens area
	Pallidum
	Caudate
Ventricles	Surface holes
	Lateral ventricle
	Choroid plexus
	Third ventricle
	Cerebrospinal fluid
	Inferior lateral ventricle
	Fourth ventricle
Corpus callosum	CC posterior
	CC mid posterior
	CC central
	CC mid anterior
	CC anterior
White matter tractography	Inferior fronto-occipital fasciculus
	Superior longitudinal fasciculus
	Temporal superior longitudinal fasciculus
	Inferior longitudinal fasciculus
	Anterior thalamic radiation
	Forceps minor
	Uncinate fasciculus
	Cingulum bundle
	Corticospinal tract
	Forceps major
	Hippocampal cingulum bundle

that did not exceed the threshold). These first level ICs were regressed from the original data before computation of the second-level ICs. Because the second level ICs had reduced statistical power (i.e., corresponded to only the remaining variance of the sample) and we used a stricter threshold of 2.0.

Overlap with "rich club" front-parietal network co-activations

To test if our ICA derived anatomical maps overlapped with the fronto-parietal "rich club" network (Jung and Haier, 2007; Van den Heuvel and Sporns, 2011), we identified the cognitive variables, anatomical segments, and white matter tracts (Table 4) implicated in this network to create a mask. We then computed the correlation between the loadings of our IC brain maps and this mask.

Results

Demographics and gross brain volumes are not strong, independent predictors of cognitive factors

Within our sample, there were no significant correlations between any of age, sex, education, or brain volume variables. Nor did these

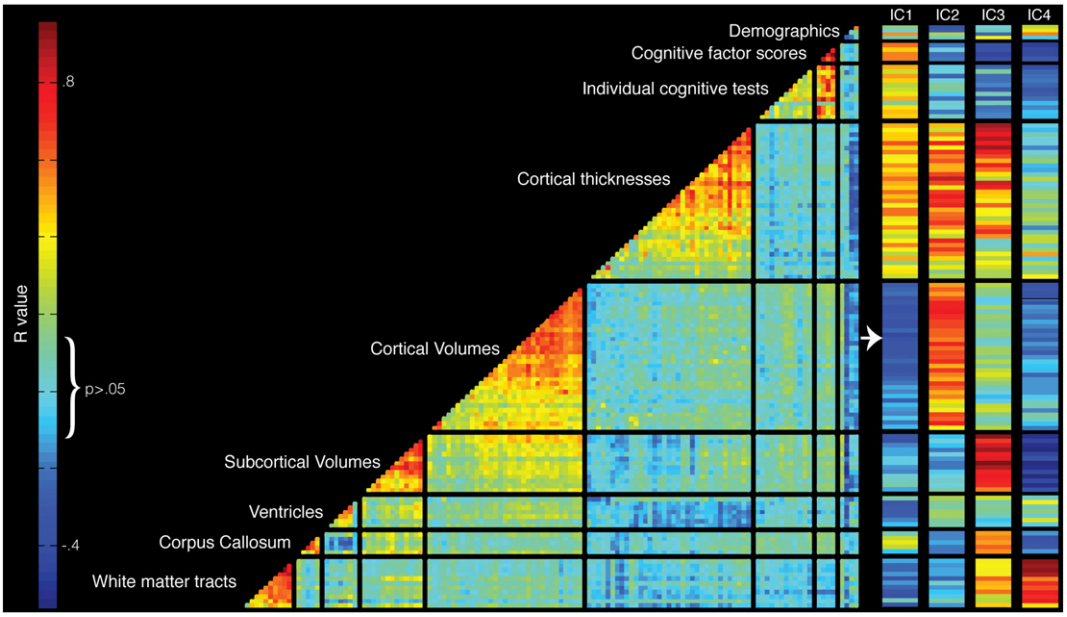

Fig. 1. Intercorrelations in multimodal imaging and cognitive data. Global correlation matrix, range of uncorrected non-significant correlations are indicated. In the global correlation matrix, interactions within similar measures (e.g., cortical thickness) exceed interactions between data types (e.g., cortical thickness and cortical volume), suggesting that these different data types are driven by a small number of underlying sources of variance. Independent component analysis (right column) decomposes the global correlations into four underlying sources of global variation.

correlate with any of the four cognitive variables with one exception: global brain volume was positively correlated with working memory ($R = .17$, $p < .03$), even when regressing out age, sex, and education variables ($R = .16$, $p < .03$).

First level ICA: correlations within anatomical and cognitive data can be characterized by independent component analysis

We computed the global correlation matrix between all measures reported in Table 3 (Fig. 1 red values are strongly positive correlations, blue strongly negative, green near 0. All R-values with a magnitude > .15 would pass an uncorrected one-sided t-test). Broadly speaking, variables were highly correlated within measurement types (i.e., demographic, cognitive factor, cognitive tests, cortical thickness, cortical volumes, subcortical volumes, ventricles, corpus callosum, and fractional anisotropy). In particular, the mean correlation within a data type was $R = .43$, $p = .07$ while across data type $R = .11$, $p = .32$. This pattern of intercorrelation suggests that the data falls into clusters, with common underlying sources of variance, and motivates our use of independent components analysis.

Scree plot inspection of the whitened data matrix and cross-validation suggested that four ICs could be reliably extracted from the global correlation matrix. Using the same color map (i.e., scaling the total range of IC values to match the total range of correlation values), we plot the four IC loadings next to the global correlation matrix (Fig. 1) to show the relative weightings of each variable on each IC. We constructed a multivariate GLM to examine the goodness of fit of the first-level ICs with the ICs as the independent variable and Table 5 as the dependent variables. Next, we projected the IC colors onto a representative brain (Fig. 2) to better visualize the spatial extent of each IC in MNI space (Mazziotta et al., 1995). Below we consider the patterns of the four first-level ICs, across anatomical and cognitive variables. While we refer to these patterns as "positive" and "negative," it should be noted that one of the limits of ICA is that components are extracted with an arbitrary sign. Thus, we emphasize the relative patterns between different measures rather than their absolute direction.

Underlying sources of variation described by first-level independent components

At the first level, variables gathered by a single measurement technique tended to group together into the first-level independent

Table 4
PFIT "rich club" network mask.

Data categories	Specific measures
Cognition	Fluid intelligence (gf)
	Working memory (wm)
	Executive function (ef)
	Episodic memory (em)
Cortical thicknesses	Superior parietal
	Precuneus
	Superior frontal
Cortical volumes	Superior frontal
	Precuneus
	Superior parietal
Sub-cortical volumes	Hippocampus
	Thalamus
	Putamen
Corpus callosum	CC mid posterior
	CC mid anterior
White matter tractography	Superior longitudinal fasciculus
	Superior longitudinal fasciculus temporal
	Anterior thalamic radiation
	Forceps minor
	Uncinate fasciculus
	Cingulum bundle
	Cingulum bundle within hippocampus

Table 5
Global variance explained by the first-level independent components.

IC1	$R^2 = .12$, $p < .001$
IC2	$R^2 = .19$, $p < .001$
IC3	$R^2 = .13$, $p < .001$
IC4	$R^2 = .15$, $p < .001$
Goodness-of-fit of the four-factor model.	$R^2 = .58$, $p < .001$

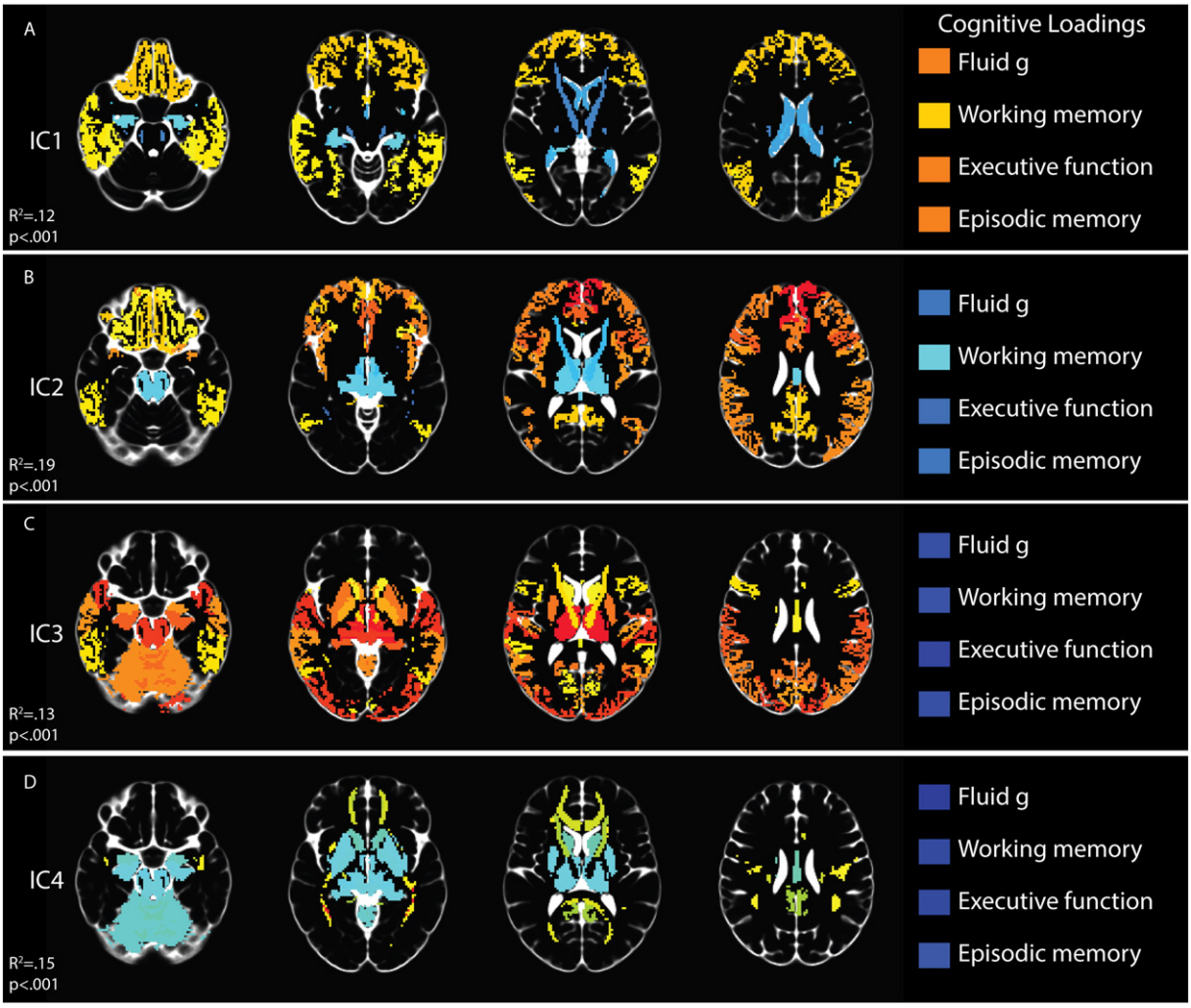

Fig. 2. First-level ICA brain maps. Projecting these four independent components (ICs) onto a representative brain in standardized MNI space shows underlying sources of variation associated with different brain regions. IC1: predominately fronto-parietal, with moderate positively loadings on cognitive factors. IC2: predominantly fronto-cortical, with slight negative loadings on all cognitive factors. IC3: posterior- and sub-cortical located with negative loadings on cognitive factors. IC4: white matter and ventricles with negative loadings on cognitive factors.

components. The two exceptions to this general pattern of uniform variation within a measurement type were demographics and cortical thicknesses. These produced a complex pattern, wherein individual variables contributed to different independent components and in different directions.

None of the four first-level components had strong loadings stemming exclusively from a single measurement type, but rather fused variation estimated by multiple converging methods. These contributions across measurement type did not clearly correspond to individual demographic variables, cognitive factors, or anatomical divisions (e.g., "frontal lobe.")

All of the first level components had cognitive loadings on all four cognitive factors that exceeded the threshold with two exceptions: the working memory factor fell below threshold on IC1 and IC2. However, only the first component (IC1) identified joint variation between cognitive and anatomical data that pointed in the same direction (i.e., greater cortical thickness implied greater cognitive scores). In all other cases, cognitive variation was negatively related to anatomical variation. Thus, we interpret these independent components (IC2–4) as being sensitive to covariance among our measures not tied to absolute magnitudes of the variables. For example, we interpret IC2 as sensitive cortical thinning across the lifespan (Salat et al., 2004; Zhou et al., 2015) having characterized and separated the independent signal of absolute brain size in IC1 and IC3.

Descriptions of each of the first-level components

The first independent component (IC1) had positive loadings for female sex, cognitive factor scores, cognitive tests, and positive loadings across several cortical thicknesses. It had negative loadings on cortical and sub-cortical volumes, ventricle size, and white matter integrity. Given the opposite anatomical relationships IC1 seems to characterize components of the cortical surface. We interpret this component in terms of the relationships between sex, brain volume, and cognitive scores. Consistent with previous literature, females have smaller brains than males, a greater proportion of gray matter, and equivalent cognitive scores (Colom et al., 2009; Goh et al., 2011; Haier et al., 2009). Thus, there must be an underlying source of joint brain and cognitive variation that models this pattern. We suggest that IC1 captures this relationship, and provides a specific map of brain regions most likely to mediate this relationship. The "brain map" projection of IC1 (Fig. 2A) showed that the positive scores related to variation in cortical thickness predominately located in fronto-parietal cortical areas, with weaker loadings on superior and middle temporal areas. This map is most

Table 6
Relationship between second analysis and main analysis.

	Main analysis IC	Age	Sex
Secondary IC1	$R^2 = .79$, $p < .001$	$R^2 = .08$, $p < .001$	$R^2 = .07$, $p < .001$
Secondary IC2	$R^2 = .53$, $p < .001$	$R^2 = .02$, $p < .07$	$R^2 = .13$, $p < .001$
Secondary IC3	$R^2 = .45$, $p < .001$	$R^2 = .05$, $p < .002$	$R^2 = .04$, $p < .01$
Secondary IC4	$R^2 = .14$, $p < .001$	$R^2 < .01$, $p = .8$	$R^2 < .01$, $p < .39$

broadly consistent with the diffuse, predominately gray matter-driven relationships between demographics, brain anatomy, and cognitive factors previously reported in the literature. We loosely refer to this component as "cortical gray matter," and note its generally positive loadings on cognitive factors.

IC2 produced strong positive loadings on a variety of cortical thickness and cortical volumes, with strong negative loadings on the demographic variables of age and years of education. It was also characterized by weak, negative loadings on cognitive factors, and sub-cortical brain volumes, including within the corpus callosum. We broadly interpret this pattern as possibly paralleling general cortical thinning that accompanies aging (Salat et al., 2004; Zhou et al., 2015). Consistent with previous literature that emphasizes greater cortical thinning in frontal regions the brain map projection of IC2 (Fig. 2B) showed especially strong positive loadings in medial frontal regions, with negative loadings in sub-cortical volumes. We loosely refer to this component as "anterior cortex." In light of this factor's negative loadings on cognitive factors we interpret it as likely indexing cortical thinning independent of overall cortical thickness.

The third independent component (IC3) had strong positive loadings on sub-cortical volumes and cortical thicknesses. It also had positive loadings on white matter tracts, both in the corpus callosum, and as assessed by fractional anisotropy. It was also the only first-level components to have a positive loading on VO_{2max} that exceeded our threshold. This component had negative loadings on female sex, and cognitive variables. As in the case of IC1, we interpret the relative direction of this relationship: males had reliably larger sub-cortical brain volumes, and a greater proportion of white matter, but did not have reliably higher cognitive variables. As with IC1, IC3's brain map projection was not uniformly distributed: it displayed greater loadings in posterior and sub-cortical brain regions (Fig. 2C). We loosely refer to this component as "subcortical gray matter," and note its relationship to overall brain size.

The final first-level component (IC4) had positive loadings on white matter tracks, and ventricles with negative loadings on cortical volumes and cognitive factors. It had positive loadings on age and education, as well as female sex. This possibly suggests that this component is sensitive to ventricular size and white matter content, and that these properties may differ by sex and age. It's negative loadings on gray matter help to explain its negative relationship to the cognitive factors. The brain map projection (Fig. 2D) shows white matter and ventricles. We loosely refer to this component as "subcortical white matter and ventricles."

Do demographic variables drive the independent component analysis?

To test if the independent components were strongly driven by the possibly non-linear contributions of the demographic variables, we repeated the IC analysis excluding these variables, but including measures of white matter integrity (i.e., radial diffusivity values for each of the white matter tracts included in the main analysis). This produced ICs similar to those produced in the original analysis. We report the correlations between the ICs computed in the main analysis and the ICs computed in the secondary analysis, as well as the relationship between the secondary ICs and the excluded demographic variables. There were strong relationships between the ICs calculated across both analyses (Table 6), suggesting that they contained similar information about individual variation. The one exception was IC4, which had originally been strongly driven by white-matter variation, as well as having strong loadings on age and sex in our original analysis. In the follow-up analysis excluding demographics, IC4 had no relationship with age or sex, and was a relatively poor model of variation associated with the original IC. This suggests that the original IC4 modeled variation predominately associated with demographic and FA values.

However, age and sex were relatively weakly related to variation on any of the ICs in the secondary analysis. This suggests that demographic measures are not strong models of the cognitive and anatomical variation captured by the ICs.

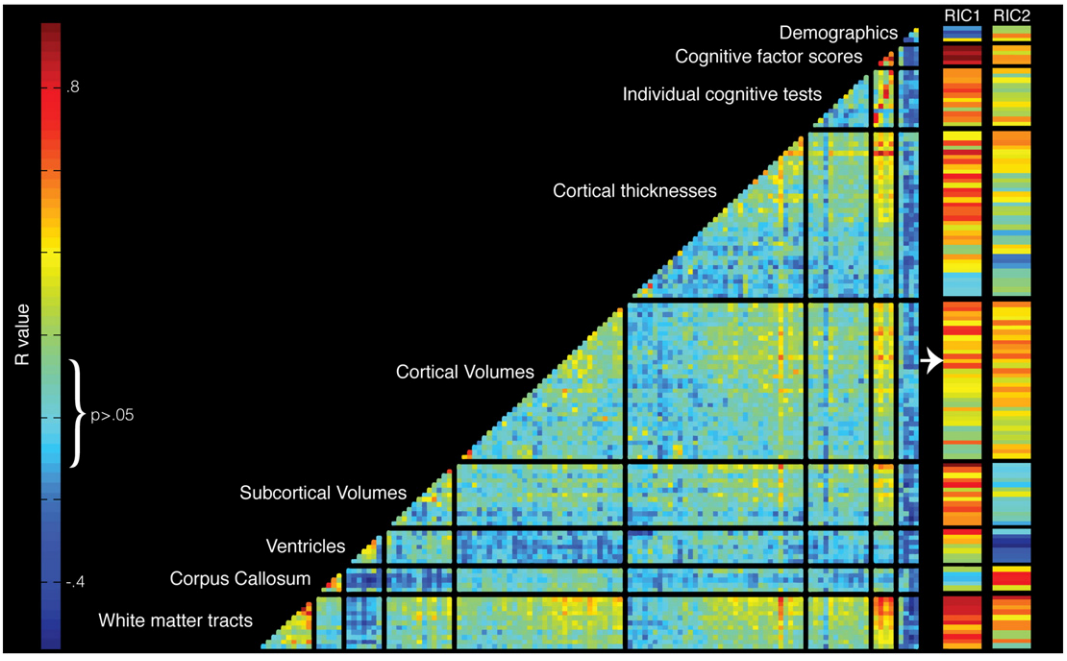

Fig. 3. Residual variation unaccounted for by first-level sources. After regressing out the effects of the first four ICs, considerable cross-domain residual correlations remain. These are decomposed into two second-level residual ICs.

Table 7
Global residual variance explained by the RICs.

RIC1	$R^2 = .08$, $p < .01$
RIC2	$R^2 = .12$, $p < .001$

Second level ICA: after accounting for first-level sources of variance, strong cognitive-brain relationships are present in residuals

Taken together, the four first-level ICs explained 58% of the cognitive and anatomical variation in our sample. We attempted to examine the residual 42% using a hierarchical approach.

To determine if there were effects beyond those captured in the first four ICs, we performed a hierarchical factor analysis. This involved a multivariate regression to compute the residuals values for each variable in our analysis partialling out effects associated with the four first-level ICs (i.e., we produced a matrix of partial correlations that accounted for the effects of the independent components). This produced a residual correlation matrix (Fig. 3). Within this matrix all relationships should be interpreted as variance unaccounted for by first-level ICs rather than as direct correlations.

This matrix had generally weaker relationships than in the original data and the strong intercorrelations that characterized the factor structure of the initial measures were absent. Instead, the strongest relationships were now across data types, suggesting that these relationships may have been obscured in the first-level analysis due to the large sources of variance associated with the four first-level ICs.

Notably, cross-modal correlations remained strong for demographic variables (in the negative direction), as well as for cognitive factors and white-matter fractional anisotropy (both in the positive direction). This suggests that the first level model including IC1-4 tends to overcorrect for variation associated with demographic variables, while failing to account for variation associated with cognitive factors and white matter. Scree plot inspection of the whitened matrix suggested that two residual ICs could be extracted from this matrix. As in the previous analysis, these were visualized beside the residual correlation matrix (Fig. 3). Goodness of fit of these residual components was also computed (Table 7).

The first factor of these residual components (RIC1) contained strong positive loadings for residual variation associated with white matter fractional anisotropy and the cognitive tests. This was especially true of the cognitive factors: the three strongest loadings on this component were the executive function, fluid g, and working memory factors.

Table 8
Correlation with rich club structures.

Independent components	Correlation with FPRCN
IC1	$R = -.05$, $p = .57$
IC2	$R = -.29$, $p < .002^*$
IC3	$R = .07$, $p = .44$
IC4	$R = .08$, $p = .36$
RIC1	$R = .29$, $p < .002^*$
RIC2	$R = .28$, $p < .002^*$

* Denotes significant results.

RIC1 produced strong negative loadings for residual variation associated with the demographic variables, age, sex and education. RIC1 also produced weaker positive loadings across distributed cortical thicknesses and subcortical volumes. The brain-map (Fig. 4A) projection showed that these positive loadings tended to cluster in positive loadings on a collection of cortical thicknesses (superior and middle frontal, inferior parietal and precuneus, superior temporal), with strong positive loadings on the white matter fiber tracts connecting those areas (e.g., superior longitudinal fasciculus and forceps minor). This pattern suggests that RIC1 index a source of variation that jointly contributes to cognition and neuroanatomy. In contrast to the P-FIT model however, superior parietal cortex was not a strong contributor to RIC1. RIC1 also included some notable, sub-cortical structures such as the cerebellum (Strick et al., 2009).

The second residual component had relatively weak loadings, only loading heavily on corpus callosum (positively), and ventricles (negatively). It had a single strong positive value in white-matter fractional anisotropy in the inferior frontal–occipital fasciculus. The brain map (Fig. 4B) suggests that RIC2 indexes variation associated with the size and shape of midline white matter and ventricles. It did not contain strong loadings on cognitive factors or tests suggesting that this component was relatively specific to anatomy.

Degree of overlap with fronto-parietal "rich club" network for first and second-level ICs

To test how well the PFIT "rich club" modeled the relationship between neuroanatomy and high-level cognitive factors, we computed correlation between the IC factor scores and the regions involved in the "rich club" (Table 8).

Of the first level ICs, only IC2 was significantly related to the fronto-parietal "rich club" network map, and this relationship was negative,

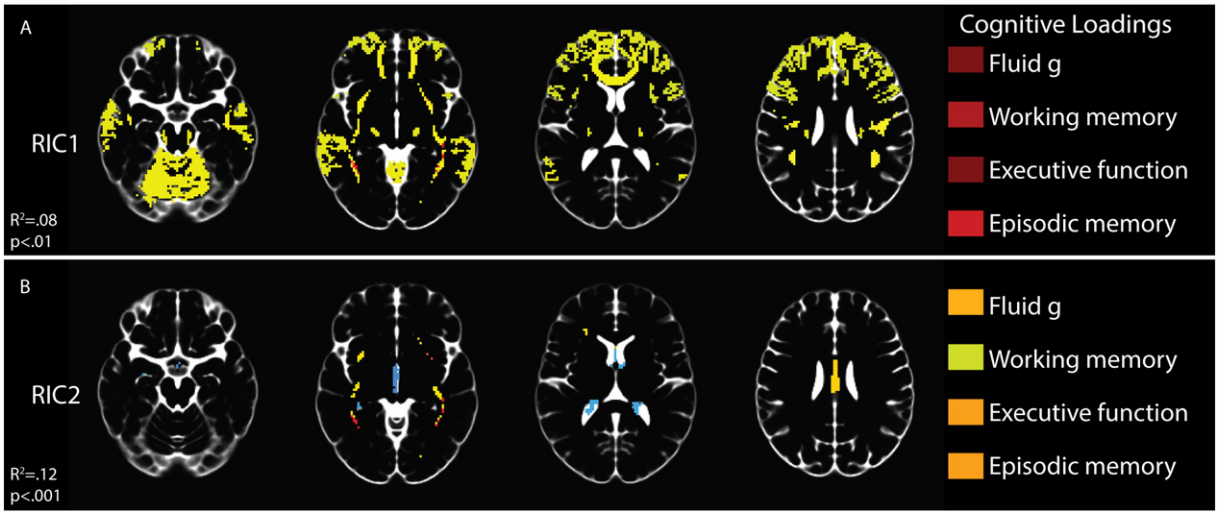

Fig. 4. Second level ICA brain maps. Projecting the two residual ICs onto a representative brain in standard space. RIC1) Has strong cognitive loadings, and a spatial profile highly similar to the "rich club" fronto-parietal control network, with especially strong weightings on white matter connectivity within this network. RIC2) no supra-threshold cognitive loadings, but some strong loadings on white matter and ventricles.

driven by negative cognitive factor loadings, and negative loadings on white matter and thalamus. However, both second-level ICs, were positively related to the PFIT rich club network. For RIC1, these relationships were driven primarily by strong loadings on white matter tracts and cognitive factors, but also by weaker loadings on cortical thicknesses in fronto-parietal regions. For RIC2, these loadings were strongly driven by white-matter tracts but more weakly driven by a variety of cortical thicknesses and cognitive factors. However, RIC2 had more diffuse loadings, most of which fell below our factor score threshold suggesting that this may be a less reliable pattern than that of RIC1.

Discussion

From a large number of variables collected across multiple methods, we characterized a small number of underlying, independent sources of variation using hICA in healthy young adults ($n = 190$). All of the first level sources were tied to cognitive factors, but separated the anatomical and demographic measures into 1) sex, fronto-parietal structures, 2) age, education, and anterior cortical gray matter, 3) fitness, posterior cortical and sub-cortical gray matter, and 4) sex and white matter.

At this first level, the sources of variation tied to demographic and gross morphological variables, but were even more strongly tied intercorrelations among variables measured with similar methods. What's more, these sources did not uniformly contribute across whole categories of variables, instead producing different loadings for each manifest variable. Thus, these first-level anatomical sources represent novel estimates of underlying sources of individual variation that cannot be solely explained with reference to traditional measures of individual variation (sex, age), nor by reference to specific anatomical or functional networks.

However, after controlling for these first-level sources of variation, one second-level component was, 1) strongly related to cognitive variables, 2) positively related to specific gray matter regions and white matter fiber tracts, and 3) highly overlapping with the P-FIT "rich club" functional network linked to fluid g, executive function, and working and episodic memory by functional imaging and lesion studies (Bergmann et al., 2012; Gray et al., 2003; Rypma and Prabhakaran, 2009). This residual factor, produced by a data-driven approach, provides converging evidence for the importance of these regions to cognitive function (Barbey et al., 2014; Colom et al., 2009; Luders et al., 2009; McDaniel, 2005), and unlike the first-level components it cannot be interpreted as an artifact of demographic variations or gross morphology because these sources of variance were removed in the first-level analysis. Thus, we suggest that the novel, data-driven first-level sources of variation may serve as useful controls in exploring high-level hypotheses for links between anatomical variations to cognitive function.

There are some important limitations to this approach. The independent components describe our sample, which was predominately college-aged adults, thus the raw factor loadings may not be directly applicable to other samples, especially ones with substantially different demographics. What's more, the independent components depend heavily on the variables included in the analysis, and inclusion of alternative neuroimaging measures might produce qualitatively similar, but quantitatively different outcomes (for example, we tested including radial diffusivity measures of white matter which produced slightly different estimates first-level sources, especially in our component related to white matter).

However, the ICA approach has certain limitations. It extracts components without sign making interpretation of the direction of a relationship impossible and, it assumes an underlying linear mixture of components, while some anatomical and cognitive links may be non-linear. Most critically however, ICA extracts underlying independent sources. This requires careful interpretation of their relationship to the observed variables, because these are mixtures of these underlying sources. Thus characterizing the underlying independent components in terms of their variables rather than variables in terms of their sources can produce incorrect interpretations.

An important example of this is the predominately negative relationships between anatomical and cognitive factors in the first level ICs. One of these is easily interpretable: IC4 loaded positively on ventricles and negatively on cognitive factors suggesting larger ventricles are related to lower cognitive scores. However, IC2 and IC3 have positive loadings on cortical and subcortical volumes, but negative loadings on cognitive factors. We do not interpret this as more brain leading to poorer cognition. Each manifest variable is the result of a mixture of the ICs, and thus variable-level interpretations must involve reference to all of the underlying ICs. For example, given its loading on a wide variety of volumetric measures as well as sex, we suggested that IC3 might represent a gross brain size. However, since males have reliably larger heads, but not reliably higher cognitive factors, some underlying source of variation ought to be positively related to brain size but negatively related to cognitive variables. The positive co-variation between brain and cognitive variables was already captured by IC1, IC4, and the residual ICs. Similarly, our interpretation of IC2's negative relationship between cortical areas and cognitive factors is that IC2 models cortical variation unaccounted for by an individual's global pattern of cortical thickness (best modeled by IC1), or volumetrics. Given the age loading on IC2 (and recent literature showing age-related cortical thinning in adolescence and early adulthood Zhou et al., 2015; Raz et al., 2005, Schuff et al., 2012), we suggested that IC2 might represent age-related changes in cortex, but it could also model variation related to brain injury or disease processes that would ordinarily be masked by ordinary anatomical variation.

This care is especially warranted when interpreting the second-level residual components. While it was tied to variation within the P-FIT network model, RIC1 explains only 8% of the residual variation in our sample, while the four first-level factors explained 58% of the total variation across 124 measures of individual difference. We did not observe sources in our sample that modeled links between specific cognitive tests and specific anatomical correlates. Nor were the novel sources of individual variation well captured by traditional measures of individual difference such as age and sex. Rather, we observed broad patterns of individual difference characterized by multiple underlying sources of variance that cut across whole categories of cognitive and anatomical factors in complex patterns.

Taken together, these results have implications for any study seeking to control for individual brain variability or exploring links between specific cognitive functions to and specific anatomical correlates. Our results suggest that individual variability in brain and cognitive function cannot be reliably accounted with a simple linear model including a small number of manifest variables such as age, sex, and brain size. Brains also vary in reliable ways over multiple dimensions of size, shape, and connectivity each of which contributes in predictable ways to covariation across anatomical regions and cognitive abilities. Additionally, while specific cognitive-anatomical correlations are undoubtedly present, they are rarely independent of these broad underlying sources of individual variation and should be interpreted as such.

We suggest that data-driven approaches, such as the one used here, can be an appropriate tool for generating robust models of the underlying sources of individual difference within a large sample and for identifying specific neuroanatomical-cognitive links that are not well characterized by these first-level sources. We were able to identify joint sources of anatomical and cognitive variation at multiple levels broadly consistent with previous functional and lesion literature on the distributed nature of high-level cognitive abilities including with areas of the core "rich club," fronto-parietal network, and the white matter tracts that form the anatomical basis for functional communications within this network (Engle et al., 1999a; Barbey et al., 2014).

We see the current result as part of the general trend toward increasingly data-driven multivariate, multi-modal neuroimaging approaches aimed at discovering broad, multi-voxel, network level

interactions tied to cognitive performance (Biswal et al., 2010). As MRI-assessed anatomical data sets grow, such data-driven approaches can produce increasingly precise and reliable characterizations of the underlying factors—anatomical and cognitive—that combine to make each brain unique.

Conclusion

We identified sources of individual variation in healthy adults across multiple measures and multiple levels using a hierarchical independent component analysis. At the first level, these components largely corresponded to strong intercorrelations within data types, as well as broad effects of demographics, cognitive factors, and anatomy. Controlling for first-level effects identified strong joint cognitive-anatomical second-level factors, particularly in white matter tracts connecting regions in the fronto-parietal "rich club." However, this second-level component explained a relatively small amount of individual variation. This approach suggests that there are a small number of underlying sources of individual variation that contribute to a wide variety of anatomical and cognitive variables. Multivariate data-driven approaches are likely more appropriate for identifying, and controlling for cognitive and brain variation at multiple levels.

Acknowledgments

This research was supported by the Intelligence Advanced Research Projects Activity (IARPA) via contract # 2014-13121700004 to the University of Illinois at Urbana–Champaign (PI: Dr. Aron Barbey). The United States Government is authorized to reproduce and distribute reprints for governmental purposes notwithstanding any copyright annotation thereon. The views and conclusions contained herein are those of the authors and should not be interpreted as necessarily representing the official policies or endorsements, either expressed or implied, of IARPA, the Office of the Director of National Intelligence, or the U.S. Government.

University of Illinois at Urbana–Champaign, Institutional Review Board study approval number 14212.

Appendix A. Supplementary data

Supplementary data to this article can be found online at http://dx.doi.org/10.1016/j.neuroimage.2016.01.023.

References

Allen, J.S., Tranel, D., Bruss, J., Damasio, H., 2006. Correlations between regional brain volumes and memory performance in anoxia. J. Clin. Exp. Neuropsychol. 28 (4), 457–476. http://dx.doi.org/10.1080/13803390590949287.

American College of Sports Medicine, 2014. ACSM's Guidelines for Exercise Testing and Prescription. nineth ed. Wolters Kluwer/Lippincott Williams & Wilkins.

Andersson, J.L.R., Jenkinson, M., Smith, S., 2007. Non-linear registration aka spatial normalisation FMRIB technial report TR07JA2. In practice. Retrieved from http://fmrib.medsci.ox.ac.uk/analysis/techrep/tr07ja2/tr07ja2.pdf.

Barbey, A.K., Colom, R., Solomon, J., Krueger, F., Forbes, C., Grafman, J., 2012. An integrative architecture for general intelligence and executive function revealed by lesion mapping. Brain 135, 1154–1164.

Barbey, A.K., Colom, R., Paul, E.J., Grafman, J., 2014. Architecture of fluid intelligence and working memory revealed by lesion mapping. Brain Struct. Funct. 219 (2), 485–494. http://dx.doi.org/10.1007/s00429-013-0512-z.

Bergmann, H.C., Rijpkema, M., Fernández, G., Kessels, R.P.C., 2012. Distinct neural correlates of associative working memory and long-term memory encoding in the medial temporal lobe. NeuroImage 63 (2), 989–997. http://dx.doi.org/10.1016/j.neuroimage.2012.03.047.

Bernreuter, R.G., Goodman, C.H., 1941. A study of the thurstone primary mental abilities tests applied to freshman engineering students. J. Educ. Psychol. 32 (1), 55–60.

Biswal, B.B., Mennes, M., Zuo, X.-N., Gohel, S., Kelly, C., Smith, S.M., ... Milham, M.P., 2010. Toward discovery science of human brain function. Proc. Natl. Acad. Sci. U. S. A. 107 (10), 4734–4739. http://dx.doi.org/10.1073/pnas.0911855107.

Bocumer Matrizentest: BOMAT-advanced-short Version. Göttingen, Hogrefe.

Buckner, R.L., Andrews-Hanna, J.R., Schacter, D.L., 2008. The brain's default network: anatomy, function, and relevance to disease. Ann. N. Y. Acad. Sci. 1124, 1–38. http://dx.doi.org/10.1196/annals.1440.011.

Colom, R., Haier, R.J., Head, K., Álvarez-Linera, J., Quiroga, M.Á., Shih, P.C., Jung, R.E., 2009. Gray matter correlates of fluid, crystallized, and spatial intelligence: testing the P-FIT model. Intelligence 37 (2), 124–135. http://dx.doi.org/10.1016/j.intell.2008.07.007.

Costello, A.B., Osborne, J.W., 1994. Denpasar declaration on population and development. Integration (40), 27–29 (doi:10.1.1.110.9154).

Dale, A.M., Fischl, B., Sereno, M.I., 1999. Cortical surface-based analysis. I. Segmentation and surface reconstruction. NeuroImage 9 (2), 179–194. http://dx.doi.org/10.1006/nimg.1998.0395.

Desikan, R.S., Ségonne, F., Fischl, B., Quinn, B.T., Dickerson, B.C., Blacker, D., ... Killiany, R.J., 2006. An automated labeling system for subdividing the human cerebral cortex on MRI scans into gyral based regions of interest. NeuroImage 31 (3), 968–980. http://dx.doi.org/10.1016/j.neuroimage.2006.01.021.

Ekstrom, R., French, J., Harman, H., & Dermen, D. (1976). Manual for kit of factor-referenced cognitive tests. Princeton NJ Educational Testing Service, 102(41), 117. doi:http://dx.doi.org/10.1073/pnas.0506897102

Engle, R.W., Tuholski, S.W., Laughlin, J.E., Conway, A.R.A., 1999a. Working Memory, Short-term Memory, and General Fluid Intelligence: A Latent-variable Approach.

Engle, R.W., Tuholski, S.W., Laughlin, J.E., Conway, A.R.A., 1999b. Working memory, short-term memory, and general fluid intelligence: a latent-variable approach. J. Exp. Psychol. Gen. 128 (3), 309–331.

Fischl, B., Dale, A.M., 2000. Measuring the thickness of the human cerebral cortex from magnetic resonance images. Proc. Natl. Acad. Sci. U. S. A. 97 (20), 11050–11055. http://dx.doi.org/10.1073/pnas.200033797.

Fischl, B., Salat, D.H., Busa, E., Albert, M., Dieterich, M., Haselgrove, C., ... Dale, A.M., 2002. Whole brain segmentation: automated labeling of neuroanatomical structures in the human brain. Neuron 33 (3), 341–355. http://dx.doi.org/10.1016/S0896-6273(02)00569-X.

Fischl, B., Salat, D. H., Van Der Kouwe, A. J. W., Makris, N., Ségonne, F., Quinn, B. T., & Dale, A. M. (2004a). Sequence-independent segmentation of magnetic resonance images. In NeuroImage (Vol. 23). doi:http://dx.doi.org/10.1016/j.neuroimage.2004.07.016

Fischl, B., Van Der Kouwe, A., Destrieux, C., Halgren, E., Ségonne, F., Salat, D.H., ... Dale, A.M., 2004b. Automatically parcellating the human cerebral cortex. Cereb. Cortex 14 (1), 11–22. http://dx.doi.org/10.1093/cercor/bhg087.

Garavan, H., 1998. Serial attention within working memory. Mem. Cogn. 26 (2), 263–276. http://dx.doi.org/10.3758/BF03201138.

Goh, S., Bansal, R., Xu, D., Hao, X., Liu, J., Peterson, B.S., 2011. Neuroanatomical correlates of intellectual ability across the life span. Dev. Cogn. Neurosci. 1 (3), 305–312. http://dx.doi.org/10.1016/j.dcn.2011.03.001.

Gray, J.R., Chabris, C.F., Braver, T.S., 2003. Neural mechanisms of general fluid intelligence. Nat. Neurosci. 6 (3), 316–322. http://dx.doi.org/10.1038/nn1014.

Groves, A.R., Beckmann, C.F., Smith, S.M., Woolrich, M.W., 2011. Linked independent component analysis for multimodal data fusion. NeuroImage 54 (3), 2198–2217. http://dx.doi.org/10.1016/j.neuroimage.2010.09.073.

Haier, R.J., Jung, R.E., Yeo, R.a., Head, K., Alkire, M.T., 2004. Structural brain variation and general intelligence. NeuroImage 23 (1), 425–433. http://dx.doi.org/10.1016/j.neuroimage.2004.04.025.

Haier, R.J., Colom, R., Schroeder, D.H., Condon, C.a., Tang, C., Eaves, E., Head, K., 2009. Gray matter and intelligence factors: is there a neuro-g? Intelligence 37 (2), 136–144. http://dx.doi.org/10.1016/j.intell.2008.10.011.

Hyvärinen, A., 1999. Fast and robust fixed-point algorithms for independent component analysis. IEEE Trans. Neural Netw. 10 (3), 626–634. http://dx.doi.org/10.1109/72.761722.

Jung, R.E., Haier, R.J., 2007. The parieto-frontal integration theory (P-FIT) of intelligence: converging neuroimaging evidence. Behav. Brain Sci. 30 (2), 135–154. http://dx.doi.org/10.1017/S0140525X07001185 (discussion 154–187).

Kane, M.J., Hambrick, D.Z., Tuholski, S.W., Wilhelm, O., Payne, T.W., Engle, R.W., 2004. The generality of working memory capacity: a latent-variable approach to verbal and visuospatial memory span and reasoning. J. Exp. Psychol. Gen. 133 (2), 189–217. http://dx.doi.org/10.1037/0096-3445.133.2.189.

Kramer, A.F., Hahn, S., McAuley, E., Cohen, N.J., Banich, M.T., Harrison, C.R., ... Vakil, E., 2001. Exercise, aging, and cognition: Healthy body, healthy mind? Human Factors Interventions for the Health Care of Older Adults

Kramer, A.F., Colcombe, S.J., McAuley, E., Scalf, P.E., Erickson, K.I., 2005. Fitness, aging and neurocognitive function. Neurobiol. Aging 26. http://dx.doi.org/10.1016/j.neurobiolaging.2005.09.009.

Laird, A.R., Fox, P.M., Eickhoff, S.B., Turner, J.A., Ray, K.L., McKay, D.R., ... Fox, P.T., 2011. Behavioral interpretations of intrinsic connectivity networks. J. Cogn. Neurosci. http://dx.doi.org/10.1162/jocn_a_00077.

Luders, E., Narr, K.L., Thompson, P.M., Toga, A.W., 2009. Neuroanatomical correlates of intelligence. Intelligence 37 (2), 156–163. http://dx.doi.org/10.1016/j.intell.2008.07.002.

Mazziotta, J.C., Toga, A.W., Evans, A., Fox, P., Lancaster, J., 1995. A probabilistic atlas of the human brain: theory and rationale for its development. The international consortium for brain mapping (ICBM). NeuroImage 2 (2), 89–101. http://dx.doi.org/10.1006/nimg.1995.1012.

McDaniel, M.a., 2005. Big-brained people are smarter: a meta-analysis of the relationship between in vivo brain volume and intelligence. Intelligence 33 (4), 337–346. http://dx.doi.org/10.1016/j.intell.2004.11.005.

Morey, R.A., Petty, C.M., Xu, Y., Hayes, J.P., Wagner, H.R., Lewis, D.V., ... McCarthy, G., 2009. A comparison of automated segmentation and manual tracing for quantifying hippocampal and amygdala volumes. NeuroImage 45 (3), 855–866.

Raz, N., Lindenberger, U., Rodrigue, K.M., Kennedy, K.M., Head, D., Williamson, A., Acker, J.D., 2005. Regional brain changes in aging healthy adults: general trends, individual differences and modifiers. Cereb. Cortex 15 (11), 1676–1689.

Rueckert, D., Sonoda, L.I., Hayes, C., Hill, D.L., Leach, M.O., Hawkes, D.J., 1999. Nonrigid registration using free-form deformations: application to breast MR images. IEEE Trans. Med. Imaging 18 (8), 712–721. http://dx.doi.org/10.1109/42.796284.

Rypma, B., Prabhakaran, V., 2009. When less is more and when more is more: the mediating roles of capacity and speed in brain-behavior efficiency. Intelligence 37 (2), 207–222. http://dx.doi.org/10.1016/j.intell.2008.12.004.

Salat, D.H., Buckner, R.L., Snyder, A.Z., Greve, D.N., Desikan, R.S.R., Busa, E., ... Fischl, B., 2004. Thinning of the cerebral cortex in aging. Cereb. Cortex 14 (7), 721–730. http://dx.doi.org/10.1093/cercor/bhh032.

Schuff, N., Tosun, D., Insel, P.S., Chiang, G.C., Truran, D., Aisen, P.S., Jack, C.R., Weiner, M.W., Alzheimer's Disease Neuroimaging Initiative, 2012. Nonlinear time course of brain volume loss in cognitively normal and impaired elders. Neurobiol. Aging 33 (5), 845–855.

Shah, P., Miyake, A., 1996. The separability of working memory resources for spatial thinking and language processing: an individual differences approach. J. Exp. Psychol. Gen. 125 (1), 4–27 (Retrieved from http://www.ncbi.nlm.nih.gov/pubmed/8851737).

Smith, S.M., 2002. Fast robust automated brain extraction. Hum. Brain Mapp. 17 (3), 143–155. http://dx.doi.org/10.1002/hbm.10062.

Smith, S.M., Jenkinson, M., Woolrich, M.W., Beckmann, C.F., Behrens, T.E.J., Johansen-Berg, H., ... Matthews, P.M., 2004. Advances in functional and structural MR image analysis and implementation as FSL. NeuroImage 23 (Suppl 1), S208–S219.

Smith, S.M., Jenkinson, M., Johansen-Berg, H., Rueckert, D., Nichols, T.E., Mackay, C.E., ... Behrens, T.E.J., 2006. Tract-based spatial statistics: voxelwise analysis of multi-subject diffusion data. NeuroImage 31 (4), 1487–1505. http://dx.doi.org/10.1016/j.neuroimage.2006.02.024.

Smith, S.M., Fox, P.T., Miller, K.L., Glahn, D.C., Fox, P.M., Mackay, C.E., ... Beckmann, C.F., 2009. Correspondence of the brain's functional architecture during activation and rest. Proc. Natl. Acad. Sci. U. S. A. 106 (31), 13040–13045. http://dx.doi.org/10.1073/pnas.0905267106.

Strick, P.L., Dum, R.P., Fiez, J.A., 2009. Cerebellum and nonmotor function. Annu. Rev. Neurosci. 32, 413–434.

Stroop, J.R., 1935. Studies of interference in serial verbal reactions. J. Exp. Psychol. http://dx.doi.org/10.1037/h0054651.

Sui, J., Pearlson, G., Caprihan, A., Adali, T., Kiehl, K.a., Liu, J., ... Calhoun, V.D., 2011. Discriminating schizophrenia and bipolar disorder by fusing fMRI and DTI in a multimodal CCA+ joint ICA model. NeuroImage 57 (3), 839–855. http://dx.doi.org/10.1016/j.neuroimage.2011.05.055.

Sui, J., Adali, T., Yu, Q., Chen, J., Calhoun, V.D., 2012. A review of multivariate methods for multimodal fusion of brain imaging data. J. Neurosci. Methods 204 (1), 68–81. http://dx.doi.org/10.1016/j.jneumeth.2011.10.031.

Unsworth, N., Redick, T.S., Heitz, R.P., Broadway, J.M., Engle, R.W., 2009. Complex working memory span tasks and higher-order cognition: a latent-variable analysis of the relationship between processing and storage. Memory (Hove, Engl.) 17 (6), 635–654. http://dx.doi.org/10.1080/09658210902998047.

Uttl, B., Graf, P., Richter, L.K., 2002. Verbal paired associates tests limits on validity and reliability. Arch. Clin. Neuropsychol. 17 (6), 567–581. http://dx.doi.org/10.1016/S0887-6177(01)00135-4.

Van den Heuvel, M.P., Sporns, O., 2011. Rich-club organization of the human connectome. J. Neurosci. 31 (44), 15775–15786. http://dx.doi.org/10.1523/JNEUROSCI.3539-11.2011.

Wang, Z., Chen, L.M., Négyessy, L., Friedman, R.M., Mishra, A., Gore, J.C., Roe, A.W., 2013. The relationship of anatomical and functional connectivity to resting-state connectivity in primate somatosensory cortex. Neuron 78 (6), 1116–1126. http://dx.doi.org/10.1016/j.neuron.2013.04.023.

Westad, F., Kermit, M., 2003. Cross validation and uncertainty estimates in independent component analysis. Anal. Chim. Acta 490 (1–2), 341–354. http://dx.doi.org/10.1016/S0003-2670(03)00090-4.

Wickett, J.C., Vernon, P. a, Lee, D.H., 2000. Relationships between factors of intelligence and brain volume. Personal. Individ. Differ. 29 (6), 1095–1122. http://dx.doi.org/10.1016/S0191-8869(99)00258-5.

Yntema, D.B., 1963. Keeping track of several things at once. Hum. Factors J. Hum. Factors Ergon. Soc. 5 (1), 7–17. http://dx.doi.org/10.1177/001872086300500102.

Zhou, D., Lebel, C., Treit, S., Evans, A., Beaulieu, C., 2015. Accelerated longitudinal cortical thinning in adolescence. NeuroImage 104, 138–145.